

Mono- and Bi-nuclear Copper(II) Complexes of Azaparacyclophanes with a Single Aromatic Spacer. Crystal Structure of $[\text{Cu}_2\text{L}^2\text{Cl}_4]\cdot 1.5\text{H}_2\text{O}$ ($\text{L}^2 = 2,5,8,11\text{-Tetraaza}[12]\text{paracyclophane}$)[†]

Antonio Andrés,^a Carla Bazzicaluppi,^b Antonio Bianchi,^b Enrique García-España,^a Santiago V. Luis,^c Juan F. Miravet^c and José A. Ramírez^a

^a Department of Inorganic Chemistry, University of Valencia, 46100 Burjassot (Valencia), Spain

^b Department of Chemistry, University of Florence, Via Maragliano 75/77, 50144 Florence, Italy

^c Laboratory of Organic Chemistry, Department of Experimental Sciences, University Jaume I, 12080 Castellón, Spain

The protonation behaviour of the azaparacyclophanes 2,6,9,13-tetraaza[14]paracyclophane (L^1), 2,5,8,11-tetraaza[12]paracyclophane (L^2) and 2,5,8,11,14-pentaaza[15]paracyclophane (L^3) has been studied at 298.1 K in 0.15 mol dm⁻³ NaClO₄ by potentiometry, direct microcalorimetry, and ¹H and ¹³C NMR spectroscopy. The data obtained by the different techniques suggest that first protonation of L^1 and L^2 occurs mainly on the benzylic nitrogens. All three ligands form mononuclear copper(II) complexes in aqueous solution characterized by an incomplete participation of the nitrogen donors in the co-ordination to the metal ion. The ligands L^2 and L^3 also form the binuclear species $[\text{Cu}_2\text{L}^2(\text{OH})_2]^{2+}$ and $[\text{Cu}_2\text{L}^3]^{4+}$, $[\text{Cu}_2\text{L}^3(\text{OH})]^{3+}$ and $[\text{Cu}_2\text{L}^3(\text{OH})_2]^{2+}$ in solution. The crystal structure of the complex $[\text{Cu}_2\text{L}^2\text{Cl}_4]\cdot 1.5\text{H}_2\text{O}$ has been solved by X-ray crystal diffraction analysis [space group $P2_1/n$, $a = 10.625(3)$, $b = 14.014(3)$, $c = 14.952(7)$ Å, $\beta = 109.55(3)^\circ$, $Z = 4$, $R = 0.066$ and $R' = 0.066$]. Both metal ions show a distorted square-pyramidal co-ordination geometry. The basal plane is defined for each metal centre by a benzylic nitrogen atom, the adjacent nitrogen atom in the chain and two chloride ions. The apical position is occupied by another chloride from a symmetry-related molecule with a much weaker bond than those in the plane. The presence of the *para*-phenylene subunit imposes enough strain to divide the macrocyclic cavity of L^2 into two separate ethylenediamine subunits.

Dimetallic copper(II) complexes have been used widely in biomimetic chemistry of copper(II) proteins and substrate activation by metal centres.^{1,2} In order to obtain such compounds several general strategies have been followed: (i) synthesis of large macrocycles or macrobicycles with a high number of donor atoms and thus ability to incorporate more than one metal ion,³ (ii) synthesis of bis(macrocycle)s^{4,5} and (iii) use of chelating agents bridging two macrocyclic ligands.^{6,7}

We have recently reported⁸ on the synthesis of a series of new macrocyclic ligands characterized by the presence of a single aromatic spacer interrupting a polyamine chain. In previous studies⁹ we indicated that the effect of the *para*-substituted aromatic spacer was to reduce the number of co-ordinated nitrogen atoms to a single metal centre. For instance, data on stability constants for the formation of copper- and zinc(II) complexes of L^1 suggested that just three out of the four nitrogen donor atoms are involved in co-ordination to the metal centre. In this paper we extend these studies to the related azaparacyclophanes 2,5,8,11-tetraaza[12]paracyclophane (L^2) and 2,5,8,11,14-pentaaza[15]paracyclophane (L^3) and we present additional evidence for the low co-ordination achieved by this family of azaparacyclophane ligands based on spectroscopy and direct microcalorimetric measurements.

Additionally we show that the combined effects of the presence of the *para*-phenylene subunit and an appropriate bridge connecting it can yield a new route to binuclear complexes, as represented by L^2 and L^3 , binuclear complexes of which have been detected. The binuclear complex $[\text{Cu}_2\text{-}$

$\text{L}^2\text{Cl}_4]\cdot 1.5\text{H}_2\text{O}$ has been isolated and its crystal structure solved by X-ray diffraction. For L^1 , which differs from L^2 only in the length of the polyamine bridge, formation of such binuclear complexes has not been observed.

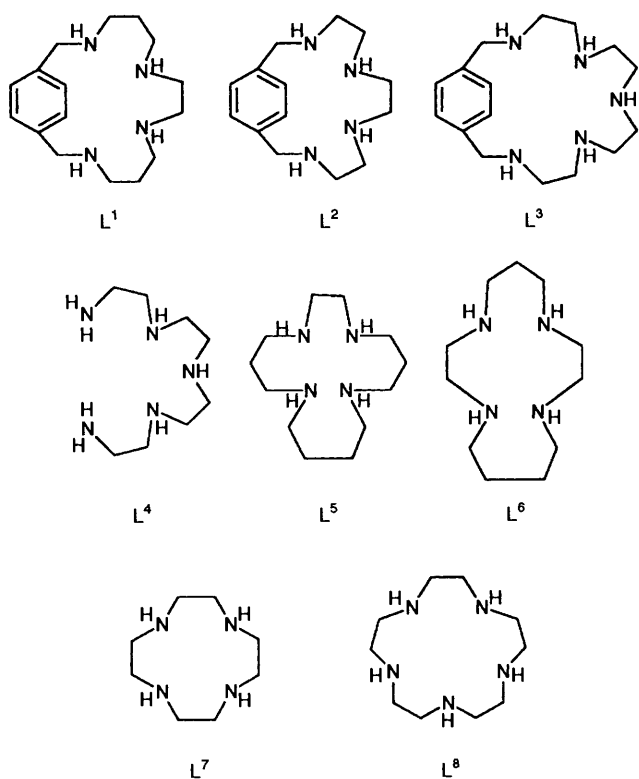
As far as we know this is the first observed formation of binuclear complexes in tetra- or penta-azamacrocycles with a continuous set of nitrogen donors linked by ethylenic chains. A similar situation for tetraazamacrocycles has just been reported where ethylenediamine subunits are separated by very long hydrocarbon chains or diethyl ether linkages.¹⁰

Experimental

Materials.—The ligands L^1 , L^2 and L^3 were synthesized as described previously^{8,9} and handled as their hydrochloride or perchlorate salts. Satisfactory elemental analysis were obtained for all the compounds. All the potentiometric measurements were carried out in 0.15 mol dm⁻³ NaClO₄, with 0.15 mol dm⁻³ NET_4ClO_4 solutions also used in some instances (see below). Sodium perchlorate was purified according to a procedure already described.¹¹ Stock solutions of $\text{Cu}(\text{ClO}_4)_2\cdot 6\text{H}_2\text{O}$ were prepared in doubly distilled water and their concentrations determined by standard gravimetric methods. Carbon dioxide free NaOH and HCl or HClO_4 solutions were prepared following the procedure reported in ref. 12. Ethylenediamine used as a tester for the microcalorimetric measurements was prepared and purified as its hydrochloride salt.

Electromotive Force Measurements.—The potentiometric titrations were carried out in 0.15 mol dm⁻³ solutions at 298.1 ± 0.1 K by using the equipment (potentiometer, burette,

[†] Supplementary data available: see Instructions for Authors, *J. Chem. Soc., Dalton Trans.*, 1994, Issue 1, pp. xxiii–xxviii.



stirrer, microcomputer, etc.) that has been fully described.¹³ The acquisition of the electromotive force (e.m.f.) data was performed with the computer program PASAT.¹⁴ The reference electrode was an Ag–AgCl electrode in saturated KCl solution; the glass electrode was calibrated as a hydrogen concentration probe by titration of well known amounts of HCl with CO₂-free NaOH solutions and determining the equivalent point by Gran's method,¹⁵ which gives the standard potential of the electrode, E° , and the ionic product of water. The program SUPERQUAD¹⁶ was employed to calculate the protonation and stability constants, and the DISPO¹⁷ program was used to obtain the distribution diagrams. At least three titration curves were performed for each one of the systems studied (ca. 200 experimental points). Concentrations of Cu²⁺ were ca. 2×10^{-3} mol dm⁻³ and those of the ligands varied from 1×10^{-3} to 1×10^{-2} mol dm⁻³, the pH range investigated was 2.5–10.0. The titration curves for each system were treated either as a single set or separately without significant variations in the values of the equilibrium constants. Furthermore, the sets of data were merged together to obtain the final values of the stability constants.

Spectroscopy.—The ¹H and ¹³C NMR spectra were recorded on Varian UNITY 300 and UNITY 400 spectrometers, operating at 299.95 and 399.95 MHz for ¹H and at 75.43 and 100.58 MHz for ¹³C, respectively. The spectra were obtained at room temperature in D₂O solutions. For the ¹³C NMR spectra dioxane was used as a reference standard (δ 67.4) and for the ¹H spectra the solvent signal. The pH was calculated from the measured pD values using the correlation, $\text{pH} = \text{pD} - 0.4$.¹⁸ The UV/VIS spectra were recorded with a Perkin-Elmer Lambda 9 spectrophotometer.

Microcalorimetry.—The enthalpies of protonation of the ligands and of complex formation were determined in 0.15 mol dm⁻³ NaClO₄ by means of an automated system composed of a Thermometric AB thermal activity monitor (model 2277) equipped with a perfusion/titration device and a Hamilton pump (model Microlab M) coupled with a gas-tight Hamilton syringe (250 cm³) (model 1750 LT). The measuring vessel was

housed in a water thermostat (25 dm³) where it was maintained at a chosen temperature within $\pm 2 \times 10^{-4}$ K. The microcalorimeter was checked by determining the enthalpy of reaction of strong base (NaOH) with strong acid (HCl). The value obtained, $-56.7(2)$ kJ mol⁻¹, was in agreement with literature values.¹⁹ Further checks were performed by determining the enthalpies of protonation of ethylenediamine. The protonation and complexation enthalpies of the ligands were determined by separate experiments. Typically, in the complexation experiments, a 5×10^{-3} mol dm⁻³ acidic solution of the ligand (1.5 cm³) in NaClO₄ (0.15 mol dm⁻³), containing Cu²⁺ (10^{-3} mol dm⁻³) was charged into the calorimetric ampoule. After thermal equilibration, additions of 0.15 mol dm⁻³ NaOH standardized solution (0.015 cm³) were delivered. Under the reaction conditions and employing the equilibrium constants determined, the concentration of each species present in solution before and after each addition were calculated and the corresponding enthalpies of reaction were determined from the calorimetric data by means of the KK88 program.²⁰ At least three titrations were performed for each system. The titration curves for each system were treated either as a single set or as separate entities without significant variations in the values of the enthalpy changes. Finally, the titration curves obtained from both protonation and complexation experiments were merged together and the corresponding enthalpies determined at the same time.

X-Ray Structure Analysis.—Crystals of [Cu₂L²Cl₄] \cdot 1.5H₂O suitable for X-ray analysis were obtained by slow evaporation of basic aqueous solutions (pH 9) of copper(II) (2×10^{-2} mol dm⁻³) and L² (10^{-2} mol dm⁻³) in the presence of an excess of chloride anions. Single crystal data were collected on an Enraf–Nonius CAD4 X-Ray diffractometer using an equatorial geometry. A prismatic blue crystal of approximate dimensions $0.2 \times 0.2 \times 0.3$ mm was mounted on the diffractometer at 25 °C with graphite-monochromated Cu–K α radiation ($\lambda = 1.5418$ Å). Cell parameters were determined by least-squares refinement of 25 carefully centred reflections. Crystal data: C₁₄H₂₇Cl₄Cu₂N₄O_{1.5}, $M = 544.3$, monoclinic, space group $P2_1/n$, $a = 10.625(3)$, $b = 14.014(3)$, $c = 14.952(7)$ Å, $\beta = 109.55(3)^\circ$, $Z = 4$, $U = 2098(1)$ Å³, $D_c = 1.72$ g cm⁻³.

The intensities of two standard reflections were monitored periodically during data collection showing no loss of intensity. A total of 3891 reflections were collected ($0 < 2\theta < 130^\circ$), intensity data were corrected for Lorentz and polarization effects, and an absorption correction was applied after structure solution.²¹ The structure was solved by the heavy-atom technique, which gave the positions of the two copper atoms. Successive Fourier-difference synthesis revealed all non-hydrogen atoms, which were refined anisotropically. The N(1)–C(1)–N(2) ethylenic chain was found to be disordered: two different models were obtained for C(1) and C(2) which were given an occupancy of 0.5 as was the oxygen atom of the water molecule. A riding model was used for the hydrogen atoms (excluding those of the water molecules), and all, except those bound to N(1), C(1), C(2) and N(2), were included in calculated positions, with an overall $U = 0.05$ Å², their coordinates refining in agreement with those atoms to which they are attached. Full-matrix least-squares refinement gave $R = 0.066$ and $R' = 0.066$ [$R = \sum |F_o| - |F_c| / \sum |F_o|$; $R' = \{ \sum w(|F_o| - |F_c|)^2 / \sum w |F_o|^2 \}^{1/2}$] for 2594 reflections having $I > 3\sigma(I)$ for 253 refined parameters. Table 1 shows the final coordinates with estimated standard deviations.

All calculations, carried out on an IBM PS/2 Model 80 computer, were performed with the SHELX 76²² set of programs which use the analytical approximation for the atomic scattering factors and anomalous dispersion corrections for all the atoms from ref. 23.

Additional material available from the Cambridge Crystallographic Data Centre comprises H-atom coordinates, thermal parameters and remaining bond lengths and angles.

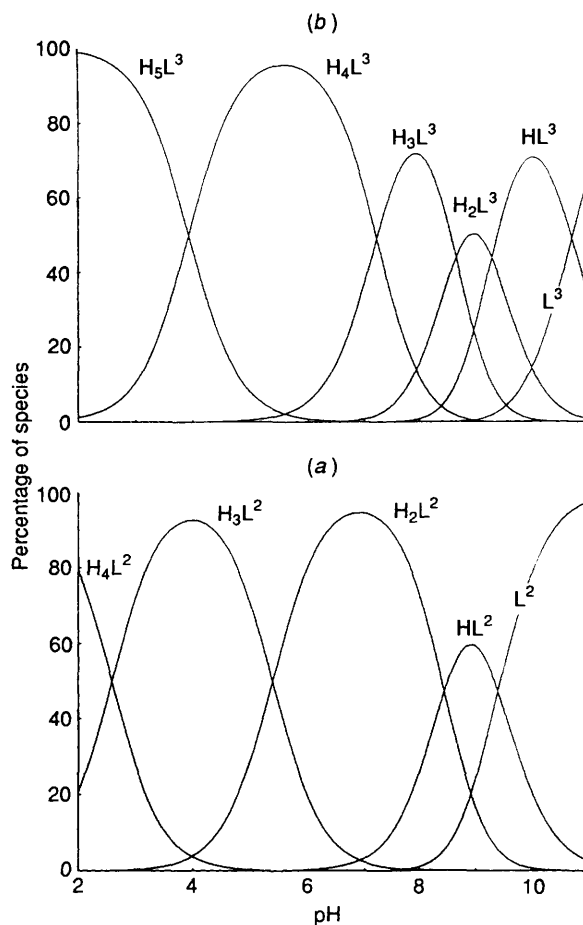
Table 1 Positional parameters ($\times 10^4$) for $[\text{Cu}_2\text{L}^2\text{Cl}_4]\cdot 1.5\text{H}_2\text{O}$, with estimated standard deviations (e.s.d.s) in parentheses

Atom	x	y	z
Cu(1)	7 529(1)	1 111(1)	5 654(1)
Cu(2)	12 205(1)	1 713(1)	9 296(1)
Cl(1)	6 533(2)	147(2)	4 364(2)
Cl(2)	9 038(2)	1 765(2)	5 076(2)
Cl(3)	13 133(2)	791(2)	10 612(2)
Cl(4)	10 632(2)	2 347(2)	9 855(2)
N(1)	13 339(7)	1 082(5)	8 624(5)
C(1)	13 555(26)	1 781(35)	7 917(28)
C(2)	12 825(25)	2 529(16)	7 758(17)
C(1')	13 017(26)	1 555(29)	7 648(21)
C(2')	12 163(18)	2 226(17)	7 372(14)
N(2)	11 651(7)	2 627(5)	8 162(5)
C(3)	10 225(9)	2 810(7)	7 604(7)
C(4)	9 370(10)	1 921(7)	7 428(8)
N(3)	8 011(7)	2 044(5)	6 763(5)
C(5)	6 944(11)	1 908(7)	7 170(7)
C(6)	6 787(9)	852(7)	7 330(7)
N(4)	6 751(6)	320(5)	6 472(5)
C(7)	7 375(8)	-638(6)	6 741(7)
C(8)	8 861(8)	-566(6)	7 159(6)
C(9)	9 647(9)	-459(6)	6 576(7)
C(10)	11 000(9)	-280(7)	6 973(7)
C(11)	11 605(8)	-222(7)	7 951(7)
C(12)	10 847(9)	-388(6)	8 537(7)
C(13)	9 489(8)	-547(6)	8 134(7)
C(14)	13 096(8)	52(7)	8 392(7)
O(1)	6 143(8)	1 469(6)	9 335(7)
O(2)	8 000(12)	2 785(7)	10 462(8)

Results and Discussion

Protonation.—Table 2 shows the logarithms of the stepwise protonation constants of the ligands L^2 and L^3 determined at 298.1 ± 0.1 K in $0.15 \text{ mol dm}^{-3} \text{ NaClO}_4$ together with those of L^1 previously reported.⁹ The protonation constants for some related tetra- and penta-azamacrocycles have also been included in Table 2 for comparison.^{24–26} The distribution diagrams for L^2 and L^3 are shown in Fig. 1. While L^2 displays two relatively basic constants, one intermediate and the last one much lower, L^3 presents three high stepwise protonation constants, an intermediate one and another one much lower. The magnitudes of the basicity constants are markedly higher for L^3 than for L^2 in each protonation step. Indeed, the value for the first protonation constant of L^3 ($\log K_1 = 10.68$) more closely resembles the values reported for related saturated tetra- and penta-aza ligands than that of L^2 ($\log K_1 = 9.39$) (see Table 2). Thus, a preliminary analysis of these data suggests that, despite the only difference in L^2 and L^3 being the presence of an additional nitrogen donor in the latter, the protonation sequences of the two ligands are different.

Usually, protonation tendencies of polyazaalkanes can be explained in terms of minimization of electrostatic repulsions as the molecule takes up protons. Accordingly, the two first protonations of L^2 and L^3 can, in principle, take place on any one of the nitrogens as long as they are not adjacent. The third proton binding L^2 is placed necessarily adjacent to one already protonated nitrogen, thus resulting in the observed drop in basicity; while the difference between the two first protonation constants is about one order of magnitude that between the second and the third one is of *ca.* three orders of magnitude. The fourth protonation obviously occurs between two polyammonium sites and consequently a further decrease in basicity is observed. For L^3 , the third protonation step can still involve nitrogens distant enough not to drastically diminish the basicity (see Scheme 1). According to the scheme accepted for other either open-chain or cyclic polyamines (see, for instance, the constants for L^4 and L^8 in Table 2), the fourth protonation of L^3 should promote an important decrease in basicity since it

**Fig. 1** Distribution diagrams for the systems $\text{H}^+ - \text{L}^2$ (a) and $\text{H}^+ - \text{L}^3$ (b)

occurs between protonated sites.²⁷ However, this is not the case and the corresponding protonation constant is still very high ($\log K = 7.23$). As this result was at first sight unexpected the effect of the background electrolyte was tested and additional titrations in 0.15 mol dm^{-3} solutions of $\text{NEt}_4\text{ClO}_4^*$ were carried out; however the results obtained in this media, although slightly different, showed a similar trend. This implies that the fourth protonation step of L^3 , involves a reorganization of the protonation sites within the molecule such that the middle nitrogen remains unprotonated and each protonated nitrogen has only one adjacent protonated site (Scheme 1). Nevertheless, the presence of the benzene cloud can provide stabilizing effects to some of the polyammonium sites as already inferred for L^1 .⁹ In this sense, the enthalpy and entropy terms directly measured by microcalorimetry for L^1 and L^2 can give useful information (Table 3). First of all, as mentioned above, the first protonation constant of L^2 is particularly low compared to other polyamines (see Table 3) and could be attributed to the effects of a particular solvation promoted by the benzene moiety. In fact, the enthalpy term associated with this protonation step is rather low ($\Delta H^\circ = -34.4 \text{ kJ mol}^{-1}$) and the entropy term ($T\Delta S^\circ = 19.7 \text{ kJ mol}^{-1}$) significantly contributes to the spontaneity of the process. For related macrocycles L^5 and L^6 the enthalpic contributions to the first protonation are considerably higher (Table 3).²⁴ Although the enthalpy term for the first protonation of L^1 is larger than that for L^2 , the relative values obtained reveal a similar tendency (see Table 3). These

* Logarithms of the stepwise protonation constants obtained for L^1 and L^3 in $0.15 \text{ mol dm}^{-3} \text{ NEt}_4\text{ClO}_4$ at 298.1 K: L^1 , $\log K_1 = 9.75(3)$, $\log K_2 = 8.90(4)$, $\log K_3 = 7.31(7)$, $\log K_4 = 3.63(8)$; L^3 , $\log K_1 = 10.53(2)$, $\log K_2 = 9.05(3)$, $\log K_3 = 8.44(4)$, $\log K_4 = 6.83(5)$, $\log K_5 = 3.20(7)$.

Table 2 Stepwise protonation constants of ligands L¹–L⁸

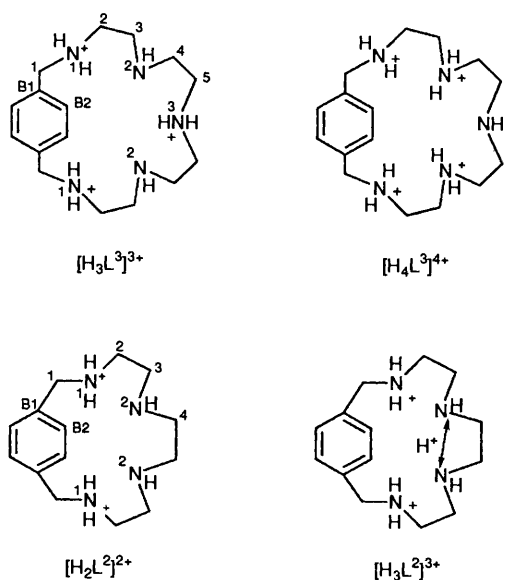
Reaction ^a	L ¹	L ²	L ³	L ⁴	L ⁵	L ⁶	L ⁷	L ⁸
H + L ⇌ HL	9.93 ^b	9.39(2) ^c	10.68(2) ^c	9.7 ^d	10.73 ^d	11.04 ^d	10.51 ^e	10.85 ^f
HL + H ⇌ H ₂ L	9.09	8.45(2)	9.29(1)	9.1	9.85	10.47	9.49	9.65
H ₂ L + H ⇌ H ₃ L	7.44	5.38(2)	8.66(2)	8.0	7.96	7.98	1.60	6.00
H ₃ L + H ⇌ H ₄ L	3.61	2.51(1)	7.23(2)	4.7	6.30	3.41	0.8	1.74
H ₄ L + H ⇌ H ₅ L			3.93(2)	3.0				1.16

^a Charges have been omitted for clarity. ^b Values taken from ref. 9, 298.1 K, 0.15 mol dm⁻³ NaClO₄. ^c This work, values determined at 298.1 ± 0.1 K in 0.15 mol dm⁻³ NaClO₄; values in parentheses are standard deviations in the last significant figure. ^d Values taken from ref. 24, 298.1 K, 0.15 mol dm⁻³ KNO₃. ^e Values taken from ref. 25, 298.1 K, 0.20 mol dm⁻³ NaClO₄. ^f Values taken from ref. 26, 298.1 K, 0.20 mol dm⁻³ NaClO₄.

Table 3 Stepwise enthalpy and entropy terms (kJ mol⁻¹) for the protonation of ligands L¹, L², L⁵ and L⁶

Reaction ^a	-ΔH°				TΔS°			
	L ¹	L ²	L ⁵	L ⁶	L ¹	L ²	L ⁵	L ⁶
H + L ⇌ HL	39.9(2) ^{b,c}	34.4(2) ^c	46.4 ^d	46.4 ^d	16.7(2) ^{b,c}	19.7(8) ^c	16.7 ^d	14.6 ^d
HL + H ⇌ H ₂ L	45.7(2)	40.5(3)	51.5	47.7	6.3(3)	7.1(5)	8.4	8.4
H ₂ L + H ⇌ H ₃ L	44.8(2)	36.6(4)	27.2	42.7	-2.5(3)	-5.8(5)	-4.6	-3.8
H ₃ L + H ⇌ H ₄ L	29.4(3)	16.7(4)	30.5	33.5	-8.8(8)	-2.1(5)	-10.9	-10.9

^a Charges have been omitted for clarity. ^b Values in parentheses are standard deviations in the last significant figure. ^c This work. ^d Values taken from ref. 24, 0.5 mol dm⁻³ KNO₃.

**Scheme 1**

data suggest that the first protonations of L¹ and L² occur on the most hydrophobic nitrogen sites of the *p*-azacyclophanes and, therefore, are accompanied by a large release of water and, consequently, involve high translational entropy.

The enthalpy terms for the next two protonations are, for both ligands, considerably higher than the first ones, the values of L¹ again being slightly higher than those for L². The magnitude of the enthalpic and entropic contributions could be dependent on the solvation of the ligands at the different protonation steps.

The enthalpy term for the fourth protonation deserves more careful analysis. The value obtained for L¹ (ΔH° = -29.4 kJ mol⁻¹) is *ca.* 12 kJ mol⁻¹ more exothermic than that of L² (ΔH° = -16.7 kJ mol⁻¹) showing the different electrostatic interactions in both molecules upon the binding of this proton. While the last protonation of L¹ occurs at a nitrogen separated from the adjacent polyammonium sites by an ethylenic and a propylenic chain, in L² the separation is just by two ethylenic chains, resulting in higher electrostatic repulsions in L² and

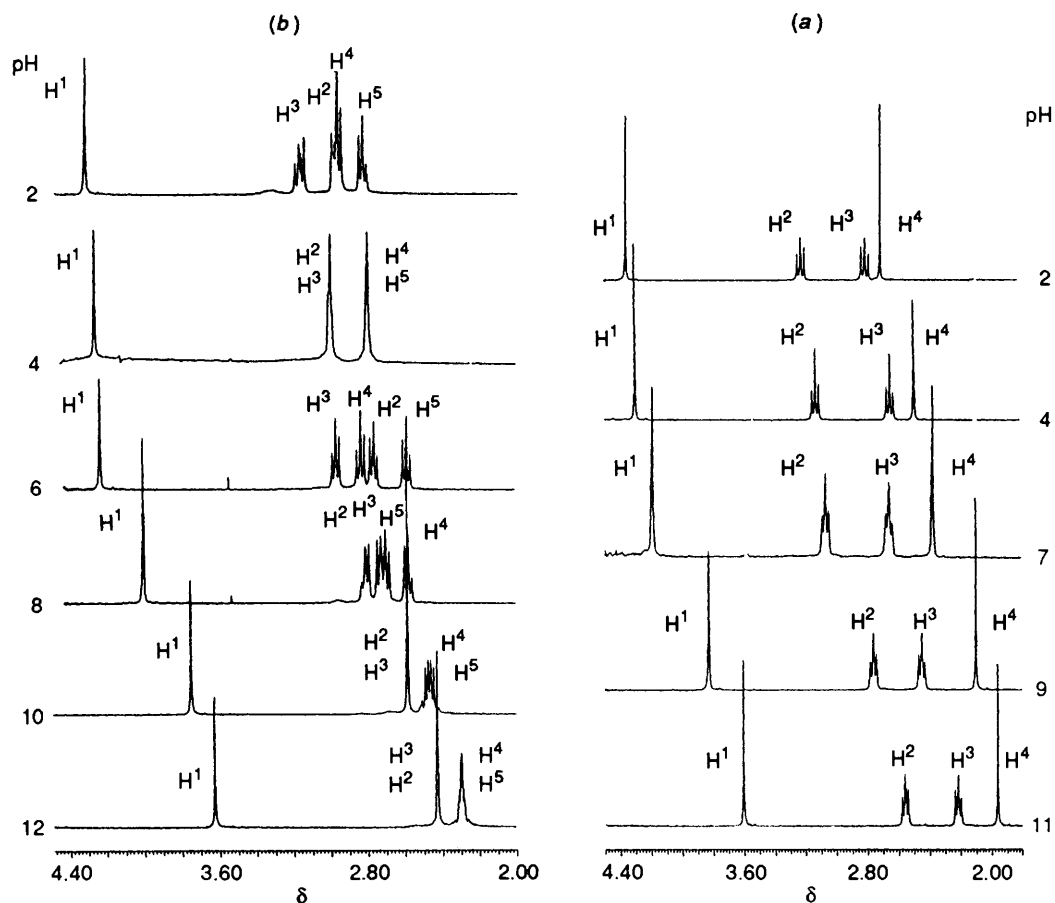
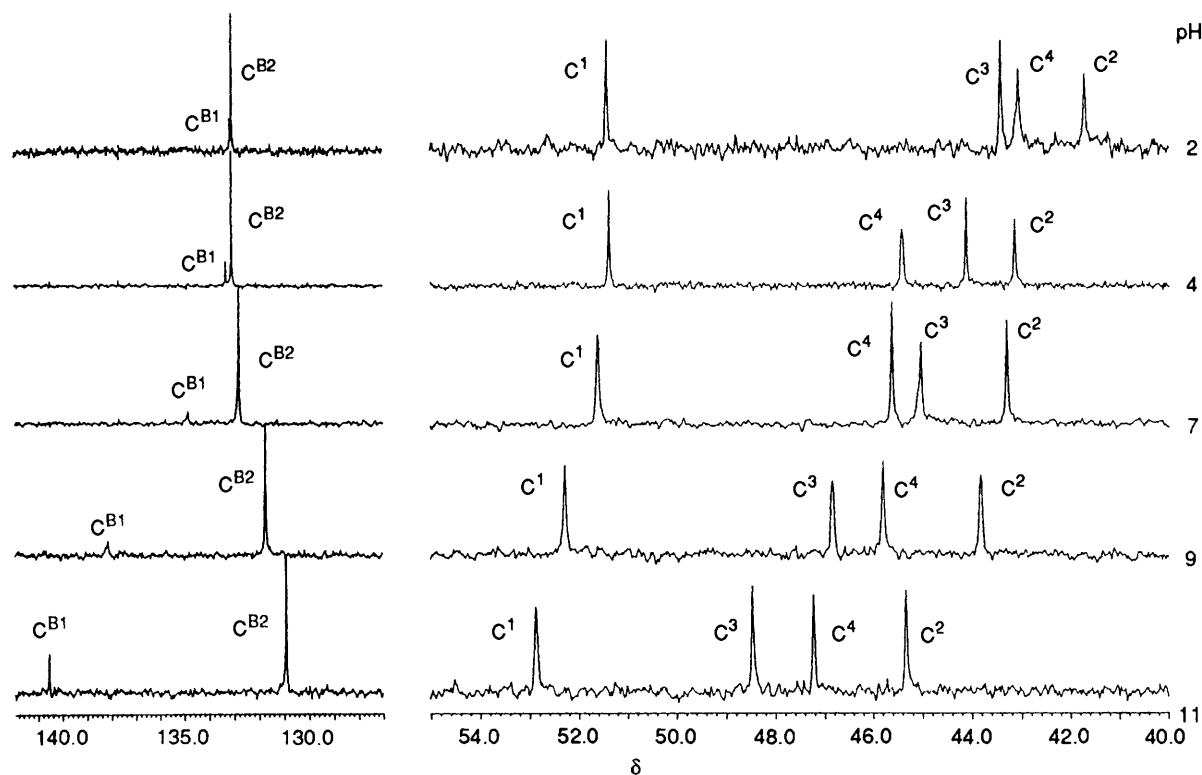
consequently a reduced exothermicity at this stage. These results are in good agreement with those in the literature for related saturated macrocycles and some of these are included in Table 3. For instance, the protonated nitrogens are separated by one ethylenic and one propylenic chain in [H₄L⁵]⁴⁺ (ΔH° = -30.5 kJ mol⁻¹) and [H₄L⁶]⁴⁺ (ΔH° = -33.5 kJ mol⁻¹) and so the enthalpy values are similar.

To obtain further insight into the protonation schemes of L² and L³ the variations of the ¹H and ¹³C NMR signals have been followed as a function of pH. All the assignments have been made on the basis of two-dimensional ¹H-¹H and ¹H-¹³C correlations at different pH values.

At pH 11 the ¹H spectrum of the free amine L² [Fig. 2(a)] shows an A₂B₂ spin-system for H² and H³ (for the numbering system see Scheme 1) (δ_A 2.22, δ_B 2.56; J_{AB} = 6.5 Hz); the protons of the middle ethylenic chain (H⁴) appear as a singlet (A₄ spin system) at δ 1.96, and the benzylic protons (H¹) as another singlet at δ 3.60. The aromatic protons (H^{B2}) display a singlet signal at δ 7.30. The ¹³C spectrum shows (Fig. 3) four signals for the aliphatic carbons C¹–C⁴ and two signals for the aromatic ones (C^{B1} and C^{B2}). Hence, the number of signals both in the ¹H and ¹³C NMR spectra indicate the presence of a binary element of symmetry in the molecule. Interestingly, C² resonates at higher field throughout the whole pH range than C³ and C⁴, probably as a result of a ring-current anisotropic effect.

Upon protonation of the molecule the spin systems do not change and only variations in the chemical shifts are observed [see Figs. 2(a) and 3]. In the pH range 7–11, where the first two protonations occur, the greatest variations in the chemical shifts are the down-field shifts experienced by protons H¹ and H², α to N¹, and the up-field shifts experienced by the quaternary aromatic carbon atoms (C^{B1}) and C³, both in a β position to N¹.²⁸ Accordingly, both first protonations presumably mainly affect the nitrogens N¹. A similar situation has already been inferred for L¹.⁹ Below pH 6, however, the largest displacements in the chemical shift correspond to protons H³ and H⁴ and carbons C² and C⁴ confirming that the last two protonations of L² mainly involve the central nitrogens (N²) (see Scheme 1).

The ¹H NMR spectrum of L³ at pH 12, where the free amine predominates, is very simple and consists of singlets either for the benzylic (H¹) or aromatic protons. The aliphatic protons H² and H³ also appear as a singlet (A₄) at this pH while

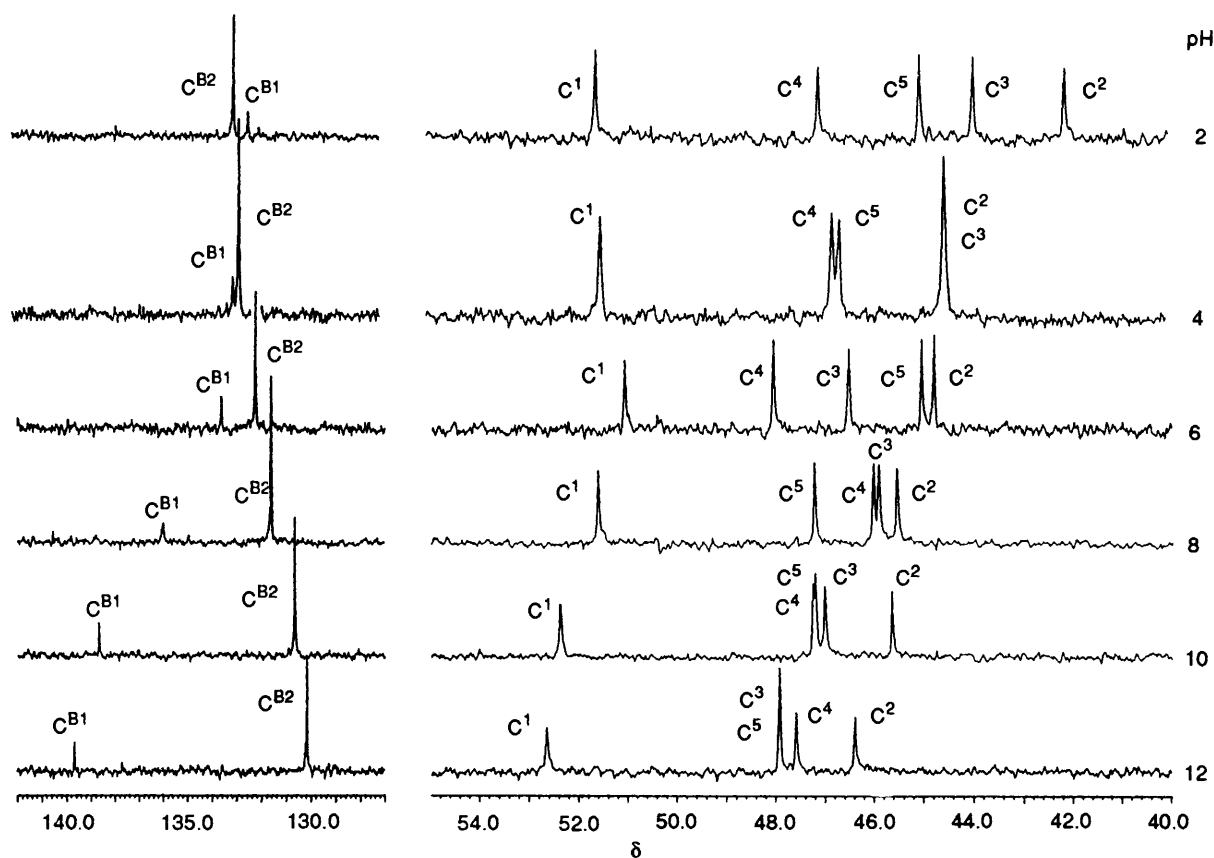
Fig. 2 ^1H NMR spectra of L^2 (a) and L^3 (b) at different pHFig. 3 ^{13}C NMR spectra of L^2 at different pH

the protons of the remaining ethylenic chain (H^4 and H^5) show an $\text{AA}'\text{BB}'$ spin system with very small differences in chemical shifts [see Table 4, Fig. 2(b)]. Since these protons are chemically non-equivalent, this is in principle quite unexpected,

particularly for H^2 and H^3 , and is probably the result of a fortuitous coincidence of chemical shifts perhaps because of the high flexibility of this molecule. However, the ^{13}C NMR spectrum shows (Fig. 4), different chemical shifts for C^2 and C^3

Table 4 Proton chemical shifts (δ) and coupling constants (J , Hz) for the system $H^+ - L^3$

pH	H^{B2}	H^1	$H^2, H^{2'}$	$H^3, H^{3'}$	$J_{2,2'} = J_{3,3'}$	$J_{2,3} = J_{2',3'}$	$J_{2,3'} = J_{2',3}$	$H^4, H^{4'}$	$H^5, H^{5'}$	$J_{4,4'} = J_{5,5'}$	$J_{4,5} = J_{4',5'}$	$J_{4,5'} = J_{4',5}$
12.0	7.249	3.615	2.417	2.417	—	—	—	2.312	2.282	-16.1	6.94	5.24
10.0	7.326	3.723	2.586	2.586	—	—	—	2.488	2.446	-16.4	6.71	6.71
8.0	7.434	4.013	2.819	2.740	-16.3	5.00	7.11	2.591	2.711	-15.9	5.70	6.77
6.0	7.521	4.236	2.763	2.969	—	5.75	—	2.834	2.586	—	6.10	—
4.0	7.530	4.281	3.003	3.003	—	—	—	2.801	2.801	—	—	—
2.0	7.544	4.332	2.978	3.173	-16.0	9.51	5.46	2.970	2.834	-16.1	6.47	5.91

**Fig. 4** ^{13}C NMR spectra of L^3 at different pH

at this pH. Owing to ring effects the signal of C^2 lies at higher field than those of the remaining ethylenic carbons (C^3 , C^4 and C^5) while C^1 is, for the same reason, very deshielded.

The analysis of variations of the chemical shifts with pH reveals several points. On going from pH 12 to pH 10, the range in which the first protonation occurs, all the 1H signals shift appreciably and while H^2 and H^3 still remain as singlets at pH 10 there is a greater difference between the chemical shifts of H^4 and H^5 than at pH 12 (see Table 4). The variations experienced by H^1 are much smaller ($\Delta\delta = 0.108$ ppm) than those observed for the analogous benzylic protons in L^1 ($\Delta\delta = 0.195$ ppm)⁹ and L^2 ($\Delta\delta = 0.228$ ppm) at this first protonation stage. The ^{13}C NMR spectrum also shows significant changes in the chemical shifts of all the carbon atoms, the largest being the variations of C^5 and C^2 (see Fig. 4). On the other hand, the upfield shift experienced by C^{B1} (β to N^1) is significantly smaller than that observed for L^2 . This could suggest that, unlike L^1 and L^2 , the first protonation of L^3 mainly affects nitrogens N^2 and N^3 in the middle of the aliphatic chains.

The 1H NMR spectrum at pH 8, where the next two protonations to yield $[H_3L^3]^{3+}$ have already occurred, shows a loss of the magnetic equivalence of protons H^2 and H^3 , which display another AA'BB' spin system [Fig. 2(b), Table 4]. The differences in chemical shift of H^4 and H^5 again increase

considerably from pH 10 to 8 and a remarkable downfield shift of the benzylic protons is observed. This, together with the upfield shifts observed for carbon atoms C^{B1} , C^3 and C^4 in the ^{13}C NMR spectrum (Fig. 4), indicates that the protons in the triprotonated form of L^3 are attached to both benzylic nitrogens N^1 and on the central nitrogen atom N^3 , which would be in accordance with the hypothesis, based on the thermodynamic data, that there is a minimum electrostatic repulsion for alternated disposition of polyammonium sites in $[H_3L^3]^{3+}$, Scheme 1.

In the pH range 8–6 a drastic change in chemical shifts occurs; while H^2 and H^5 shift upfield, H^3 and H^4 shift downfield and additionally, the spin systems of the protons of both ethylenic chains change to A_2B_2 patterns (Fig. 2, Table 4). In the ^{13}C NMR spectrum, the resonances of C^3 and C^4 move downfield while C^2 and C^5 move upfield accordingly with deprotonation of N^3 and protonation of N^2 . All these data support the reorganization depicted in Scheme 1 for $[H_4L^3]^{4+}$, and partly explain the large value obtained for the fourth successive protonation constant of L^3 .

Between pH 6 and 4, where $[H_4L^3]^{4+}$ and $[H_5L^3]^{5+}$ coexist in solution, the resonances of the carbon atoms in the same ethylenic chains collapse yielding two different singlets in the 1H NMR spectrum (A_4 spin system). This coalescence of

both ^1H and ^{13}C signals may be interpreted as a quick exchange of protons between protonated nitrogen sites within the NMR time-scale favoured by the high flexibility of L^3 .

On completion of the fifth protonation step the spin systems of the protons of both ethylenic chains change again to AA'BB' patterns accordingly with the greater rigidity of the fully protonated molecule. The ^{13}C NMR spectrum shows, at this stage (Fig. 4), upfield shifts for all the carbon atoms except C^4 and different signals for each one of the carbon atoms are observed.

Therefore the thermodynamic and NMR data for the protonation of both ligands L^2 and L^3 show the different influences of the benzene moiety depending on the length and consequent flexibility of the molecules.

Copper(II) Co-ordination Chemistry.—Table 5 shows the logarithms of the stability constants for the formation of Cu^{2+} complexes of L^2 and L^3 determined by potentiometry at 298.1 ± 0.1 K in $0.15 \text{ mol dm}^{-3} \text{ NaClO}_4$ together with those previously reported for L^1 under the same experimental conditions.⁹ For molar ratios $[\text{Cu}^{2+}]:[\text{L}] < 1:1$ the speciation model of L^2 and L^1 is similar, and in the pH range 2.5–10 formation of $[\text{Cu}(\text{HL})]^{3+}$, $[\text{CuL}]^{2+}$ and $[\text{CuL}(\text{OH})]^+$ species has been detected in both systems. However, for molar ratios $[\text{Cu}^{2+}]:[\text{L}] > 1:1$, an additional binuclear species of $[\text{Cu}_2\text{L}^2(\text{OH})_2]^{2+}$ stoichiometry has been observed, for L^1 there is no experimental evidence for the formation of binuclear species. The formation of binuclear complexes of L^2 was confirmed by UV/VIS spectrophotometric measurements. Plots of molar ratio *vs.* absorbance give a break at $[\text{Cu}^{2+}]:[\text{L}]$ 2:1 for L^2 while for L^1 a similar feature is found for a molar ratio of 1:1.

The speciation model for L^3 is somewhat different. This ligand can form up to a triprotonated mononuclear complex (see Table 5) and, on the other hand, for molar ratios $[\text{Cu}^{2+}]:[\text{L}^3] > 1:1$ an unprotonated binuclear complex $[\text{Cu}_2\text{L}^3]^{4+}$ and two hydroxylated ones, $[\text{Cu}_2\text{L}^3(\text{OH})]^{3+}$ and $[\text{Cu}_2\text{L}^3(\text{OH})_2]^{2+}$, are observed. Plots of the molar ratio as a function of absorption in the UV/VIS region also indicate the formation of binuclear species.

If we first focus our attention on the mononuclear copper(II) tetraazaparacyclophanes L^1 and L^2 , the analysis of their stabilities gives strong support to an incomplete participation of all the nitrogens in co-ordination to copper. In fact, the stabilities of the two complexes $[\text{CuL}^1]^{2+}$ and $[\text{CuL}^2]^{2+}$ (log $K = 13.02$ and 10.41 respectively) are very low compared with saturated tetraazacycloalkanes,^{9,26} and, additionally, the first

protonation constants of the complexes ($[\text{CuL}]^{2+} + \text{H}^+ \rightleftharpoons [\text{Cu}(\text{HL})]^{3+}$, log $K = 7.80$ and 6.51 for L^1 and L^2 respectively), are both higher than the third protonation constants of the unco-ordinated ligands (log $K_3 = 7.44$ and 5.38 for L^1 and L^2 respectively). The protonation constants of the doubly charged cations $[\text{ML}]^{2+}$ and $[\text{H}_2\text{L}]^{2+}$ are in agreement with protonation occurring on an unco-ordinated nitrogen atom. The UV/VIS spectra also support this since for both systems the spectra of solutions containing $[\text{Cu}(\text{HL})]^{3+}$ or $[\text{CuL}]^{2+}$ are identical (L^1 , $\lambda = 590$, $\epsilon = 180$; L^2 , $\lambda = 588$ nm, $\epsilon = 52 \text{ dm}^3 \text{ mol}^{-1} \text{ cm}^{-1}$). The thermodynamic parameters for the formation of copper(II) mononuclear complexes of L^1 and L^2 , obtained at 298.1 K in $0.15 \text{ mol dm}^{-3} \text{ NaClO}_4$ by direct microcalorimetry, are shown in Table 6. The enthalpy terms for the formation of the $[\text{CuL}^1]^{2+}$ and $[\text{CuL}^2]^{2+}$ (-49.8 and $-38.1 \text{ kJ mol}^{-1}$, respectively) are low compared with related tetraazaalkanes. For instance, the enthalpies reported for the $[\text{CuL}]^{2+}$ complexes of 1,4,8,11-tetraazacyclotetradecane and 1,4,7,10-tetraazacyclopentadecane are -126.8 and $-80.3 \text{ kJ mol}^{-1}$, respectively.^{29,30} The enthalpic contribution for L^1 , although lower, is close to that of the saturated triazamacrocycle 1,4,7-triazacyclononane ($-59.4 \text{ kJ mol}^{-1}$).³¹ The most unambiguous confirmation of the low co-ordination is provided by the enthalpic and entropic contributions to the formation equilibria of the monoprotonated complexes, $[\text{CuL}]^{2+} + \text{H} \rightleftharpoons [\text{Cu}(\text{HL})]^{3+}$ ($\Delta H^\circ = -47$ and -35 kJ mol^{-1} for L^1 and L^2), which are very close or even more exothermic than those for the first protonations of unco-ordinated L^1 ($\Delta H^\circ = -39.9$) and L^2 ($\Delta H^\circ = -34.4 \text{ kJ mol}^{-1}$). These data clearly show that protonation occurs on an unco-ordinated nitrogen. Therefore, a maximum of three out of the four nitrogen donors present in L^1 and L^2 are involved in co-ordination to Cu^{2+} . Moreover, the low stability constant and enthalpy term obtained for L^2 may even suggest that just two out of the four nitrogen donors are effectively co-ordinating the Cu^{2+} ion in this case. The higher values for the hydroxylation of the complex $[\text{CuL}^2]^{2+}$ with respect to $[\text{CuL}^1]^{2+}$ ($[\text{CuL}^2]^{2+} + \text{OH}^- \rightleftharpoons [\text{CuL}(\text{OH})]^+$: L^1 , log $K = 4.63$, $\Delta H^\circ = -7.9$; L^2 , log $K = 5.56$, $\Delta H^\circ = -16.7 \text{ kJ mol}^{-1}$), which are due to a more favourable enthalpic contribution, further support this hypothesis (Table 6). So, it seems that the presence of the *para*-phenylene subunit imposes enough strain into these molecules to avoid simultaneous co-ordination of both benzylic nitrogens to the metal centre, which suggests the possibility of facile selective functionalization of the vacant co-ordination position. Indeed we are developing this synthetic route and the results will be published elsewhere.³²

Table 5 Stability constants for the formation of copper(II) complexes by the azaparacyclophanes L^1 – L^3 determined at 298.1 ± 0.1 K in $0.15 \text{ mol dm}^{-3} \text{ NaClO}_4$

Reaction ^a	L^1	L^2	L^3
$\text{Cu} + \text{L} \rightleftharpoons [\text{CuL}]$	13.02 ^b	10.41(2) ^c	17.73(5)
$\text{Cu} + \text{L} + \text{H} \rightleftharpoons [\text{Cu}(\text{HL})]$	20.82	16.92(1)	26.86(4)
$\text{Cu} + \text{L} + 2\text{H} \rightleftharpoons [\text{Cu}(\text{H}_2\text{L})]$			33.28(2)
$\text{Cu} + \text{L} + 3\text{H} \rightleftharpoons [\text{Cu}(\text{H}_3\text{L})]$			37.65(2)
$\text{Cu} + \text{L} + \text{H}_2\text{O} \rightleftharpoons [\text{CuL}(\text{OH})] + \text{H}$	3.92	2.27(6)	6.65(6)
$[\text{CuL}] + \text{H} \rightleftharpoons [\text{Cu}(\text{HL})]$	7.80	6.51	9.13
$[\text{Cu}(\text{HL})] + \text{H} \rightleftharpoons [\text{Cu}(\text{H}_2\text{L})]$			6.42
$[\text{Cu}(\text{H}_2\text{L})] + \text{H} \rightleftharpoons [\text{Cu}(\text{H}_3\text{L})]$			4.37
$[\text{CuL}] + \text{H}_2\text{O} \rightleftharpoons [\text{CuL}(\text{OH})] + \text{H}$	-9.10	-8.14	-11.08
$[\text{CuL}] + \text{OH} \rightleftharpoons [\text{CuL}(\text{OH})]$	4.63	5.59	2.65
$2\text{Cu} + \text{L} \rightleftharpoons [\text{Cu}_2\text{L}]$			24.29(4)
$2\text{Cu} + \text{L} + \text{H}_2\text{O} \rightleftharpoons [\text{Cu}_2\text{L}(\text{OH})] + \text{H}$			16.95(4)
$2\text{Cu} + \text{L} + 2\text{H}_2\text{O} \rightleftharpoons [\text{Cu}_2\text{L}(\text{OH})_2] + \text{H}$		3.44(3)	7.50(6)
$[\text{CuL}] + \text{Cu} \rightleftharpoons [\text{Cu}_2\text{L}]$			6.56
$[\text{Cu}_2\text{L}] + \text{H}_2\text{O} \rightleftharpoons [\text{Cu}_2\text{L}(\text{OH})] + \text{H}$			-7.34
$[\text{Cu}_2\text{L}(\text{OH})] + \text{H}_2\text{O} \rightleftharpoons [\text{Cu}_2\text{L}(\text{OH})_2] + \text{H}$			-9.45

^a Charges have been omitted for clarity. ^b Values taken from ref. 9, $0.15 \text{ mol dm}^{-3} \text{ NaClO}_4$. ^c Values in parentheses are standard deviations in the last significant figure.

Table 6 Enthalpy and entropy terms (kJ mol^{-1}) for the formation of copper(II) complexes of the azaparacyclophanes L^1 and L^2 . The enthalpy terms for the protonation of the unco-ordinated ligands have also been included

Reaction ^a	L^1		L^2	
	$-\Delta H^\circ$	$T\Delta S^\circ$	$-\Delta H^\circ$	$T\Delta S^\circ$
$\text{Cu} + L \rightleftharpoons [\text{Cu}L]$	49.8(4) ^b	24.7(8)	38.1(8)	20.9(8)
$[\text{Cu}L] + \text{H} \rightleftharpoons [\text{Cu}(\text{HL})]$	47(1)	-10(1)	35(1)	0.4(9)
$L + \text{H} \rightleftharpoons \text{HL}$	39.9(2)		34.4(2)	
$[\text{Cu}L] + \text{OH} \rightleftharpoons [\text{Cu}L(\text{OH})]$	7.9(8)	18.8(8)	16.7(8)	14(1)

^a Charges have been omitted for clarity. ^b Values in parentheses are standard deviations in the last significant figure.

The situation for L^3 is somewhat different and not as easy to analyse since, unfortunately, the complexity of the system prevented the collection of sufficiently reliable calorimetric data. However, the number of protonated species formed and the values of their protonation constants again suggest incomplete co-ordination of the ligand. The stability constant obtained for $[\text{Cu}L^3]^{2+}$, $\log K = 17.73$, is low compared to related polyamines³¹ and the protonation constants are high with those for the two first protonation steps, $[\text{Cu}L^3]^{2+} + \text{H}^+ \rightleftharpoons [\text{Cu}(\text{HL}^3)]^{3+}$ and $[\text{Cu}(\text{HL}^3)]^{3+} + \text{H}^+ \rightleftharpoons [\text{Cu}(\text{H}_2\text{L}^3)]^{4+}$ ($\log K = 9.13$ and 6.42), comparing well with those for unco-ordinated L^3 displaying the same overall charges: $\text{H}_2\text{L}^{32+} + \text{H}^+ \rightleftharpoons \text{H}_3\text{L}^{33+}$; $\log K_3 = 8.66$ and $\text{H}_3\text{L}^{33+} + \text{H}^+ \rightleftharpoons \text{H}_4\text{L}^{34+}$; $\log K_4 = 7.23$. Therefore, although it is difficult to predict the correct co-ordination number in this system, it seems unlikely that all five nitrogens are involved. The data may be interpreted as resulting from co-ordination of three nitrogen atoms, or weak co-ordination from four.

Perhaps the most noticeable feature of the copper co-ordination chemistry of the azaparacyclophanes is the formation of binuclear complexes of L^2 and L^3 in aqueous solution. This is the first time that formation of such species has been reported for tetra- or penta-azamacrocycles containing a continuous set of nitrogens linked by ethylenic chains. A similar result was found for 1,10,19,28-tetraoxa-4,7,13,16,22,25,31,34-octaazacyclohexatriacontane, in which the four ethylenediamine subunits are separated by $\text{CH}_2\text{O}(\text{CH}_2)_2$ bridges.¹⁰

The crystal structure of the compound $[\text{Cu}_2L^2]\text{Cl}_4 \cdot 1.5\text{H}_2\text{O}$ (see below) shows that the combined effects of the *para*-substituted phenylene and the length of the polyamine bridge are the key points in determining the bis(chelating) properties of the ligand. In fact L^1 which differs from L^2 only in the presence of two additional carbon atoms in the bridge does not form a binuclear species, as the greater flexibility of the polyamine bridge in L^1 results in stronger co-ordination of the metal centre in the mononuclear complex therefore precluding the formation of binuclear complexes.

The low number of co-ordinated nitrogen atoms to the copper(II) centres in the binuclear complexes give rise to the formation of very stable hydroxo species as shown by the distribution of the species present in equilibrium for a ratio $[\text{Cu}^{2+}]:[\text{L}]$ of 2:1 in the $\text{Cu}^{2+}-L^2$ and $\text{Cu}^{2+}-L^3$ systems (Fig. 5). The high acidity of the water molecule co-ordinated to the binuclear complexes ($\log K = -7.34$ for the equilibrium $[\text{Cu}_2L^3]^{4+} + \text{H}_2\text{O} \rightleftharpoons [\text{Cu}_2L^3(\text{OH})]^{3+} + \text{H}^+$) may be of interest for the future application of these complexes in assisting catalytic processes.

Description of the Crystal Structure.—The molecular structure consists of discrete $[\text{Cu}_2L^2\text{Cl}_4]$ binuclear units and lattice water molecules, with the macrocyclic molecule behaving as a bis(chelating) ligand. An ORTEP³³ drawing of the

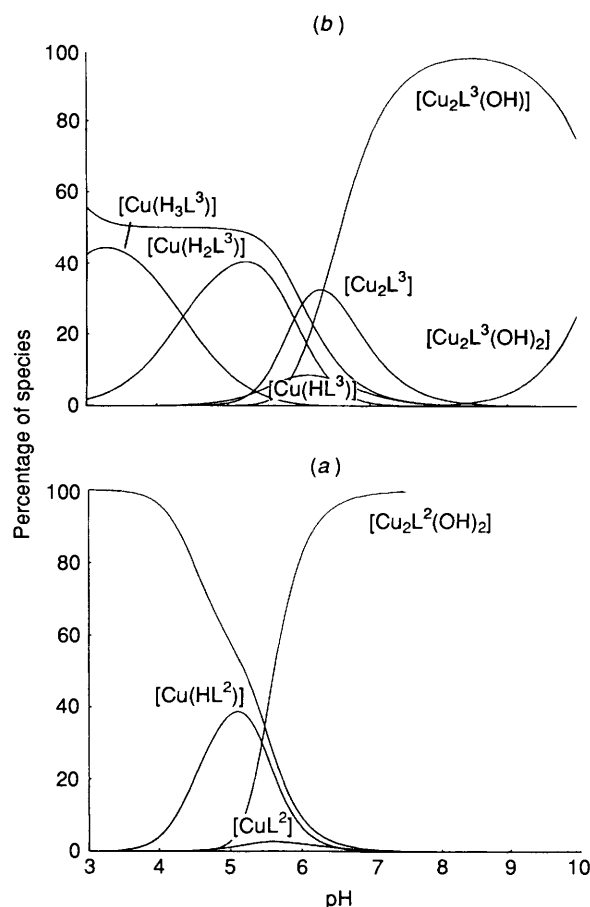


Fig. 5 Distribution diagrams for the species existing in equilibrium for the systems $\text{Cu}^{2+}-L^2$ (a) and $\text{Cu}^{2+}-L^3$ (b). $[\text{Cu}^{2+}] = 2 \times 10^{-3}$ mol dm^{-3} , $[\text{L}^2] = [\text{L}^3] = 1 \times 10^{-3}$ mol dm^{-3}

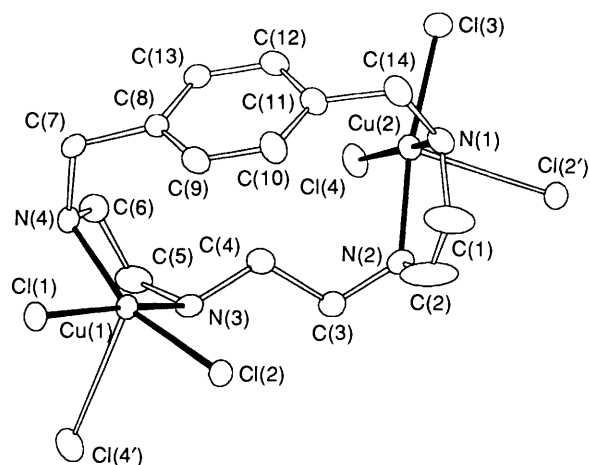


Fig. 6 An ORTEP drawing showing a single $[\text{Cu}_2L^2\text{Cl}_4]$ molecule. Thermal ellipsoids are drawn at the 50% probability level

compound is shown in Fig. 6 and some selected bond distances and angles (PARST)³⁴ are listed in Table 7.

Both metal ions, separated by $6.077(3)$ Å, show a fairly distorted square-pyramidal co-ordination geometry, strongly axially elongated. The adjacent nitrogens N(3) and N(4), together with Cl(1) and Cl(2) and the metal atom, form the basal plane of the co-ordination sphere of Cu(1) [maximum deviation 0.55 Å for N(4)].³⁴ The bond distances in the plane range from $2.021(8)$ Å, for N(4), to $2.303(2)$ Å, for Cl(1). The apical position of the pyramid is occupied by the Cl(4') atom from a symmetry-

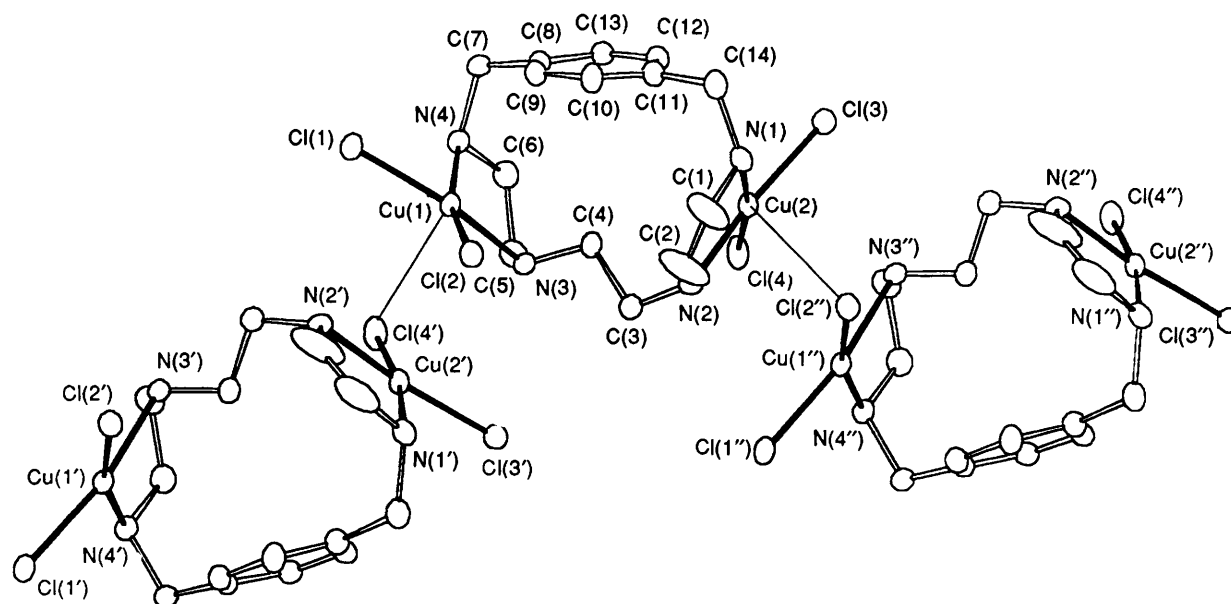


Fig. 7 An ORTEP drawing showing the polymeric-chain disposition of $[\text{Cu}_2\text{L}^2\text{Cl}_4]$. Thermal ellipsoids are drawn at the 50% probability level

Table 7 Selected bond distances (Å) and angles (°) for $[\text{Cu}_2\text{L}^2\text{Cl}_4] \cdot 1.5\text{H}_2\text{O}$ with e.s.d.s in parentheses

Cu(1)–Cl(1)	2.303(3)	Cu(2)–Cl(4)	2.283(3)
Cu(1)–Cl(2)	2.255(3)	Cu(2)–N(1)	2.014(9)
Cu(1)–N(3)	2.037(7)	Cu(2)–N(2)	2.048(7)
Cu(1)–N(4)	2.021(8)	Cu(2)–Cl(3)	2.284(3)
Cu(1)–Cl(4')	2.924(3)	Cu(2)–Cl(2')	2.860(3)
Cu(1)···Cu(2')	3.615(2)	Cu(1)···Cu(2)	6.077(3)
Cl(4')–Cu(1)–N(4)	106.7(2)	Cl(2)–Cu(1)–N(3)	92.0(2)
Cl(4')–Cu(1)–N(3)	79.0(2)	Cl(1)–Cu(1)–N(4)	91.1(2)
Cl(2)–Cu(1)–Cl(4')	91.4(9)	Cl(1)–Cu(1)–N(3)	168.0(3)
Cl(1)–Cu(1)–Cl(4')	91.8(9)	Cl(1)–Cu(1)–Cl(2)	95.9(1)
Cl(2')–Cu(2)–N(2)	80.8(2)	N(1)–Cu(2)–N(2)	85.1(3)
Cl(2')–Cu(2)–N(1)	95.2(2)	Cl(4)–Cu(2)–N(2)	91.0(2)
Cl(2')–Cu(2)–Cl(4)	92.5(9)	Cl(4)–Cu(2)–N(1)	170.7(2)
Cl(2')–Cu(2)–Cl(3)	91.8(9)	Cl(3)–Cu(2)–N(2)	171.4(2)
N(3)–Cu(1)–N(4)	84.4(3)	Cl(3)–Cu(2)–N(1)	91.4(2)
Cl(2)–Cu(1)–N(4)	160.4(2)	Cl(3)–Cu(2)–Cl(4)	93.6(1)

Symmetry relations: Cl(2') $0.5 + x, 0.5 - y, 0.5 + z$; Cl(4') $x - 0.5, y - 0.5, z - 0.5$.

related molecule. The Cu(1)–Cl(4') bond forms an angle of 1.86° with the normal to the plane.

The co-ordination sphere of Cu(2) is similar with N(1), N(2), Cl(3), Cl(4) forming the base and Cl(2') from a symmetry-related molecule occupying the apical position of an axially elongated square pyramid. The maximum deviation from the basal plane is 0.26 \AA for N(1) and the bond distances are in the range $2.014(9)$ – $2.284(3) \text{ \AA}$.

The two basal planes are perpendicular to each other, with a dihedral angle of 93.36° . The four nitrogen atoms of the ligand are nearly coplanar, the maximum deviation being 0.12 \AA for N(3), and this plane forms dihedral angles of 84.93 and 82.07° with the basal planes of the co-ordination spheres of Cu(1) and Cu(2), respectively, and 94.47° with the plane containing the aromatic ring.

The Cu–Cl axial bonds are much weaker than those in the basal planes [Cu(1)–Cl(4') $2.924(3)$ and Cu(2)–Cl(2') $2.860(3) \text{ \AA}$], these axial elongations being significantly greater than those usually found for analogous square-pyramidal copper(II) complexes.³⁵ The particular arrangement of the co-ordination spheres for both copper atoms gives rise to polymeric chains

(see Fig. 7) with the Cl(2) and Cl(4) chloride ions bridging two metal atoms of different molecules, with a Cu···Cu separation of $3.615(2) \text{ \AA}$.

Conclusion

The solution data and the crystal structure of the complex $[\text{Cu}_2\text{L}^2\text{Cl}_4] \cdot 1.5\text{H}_2\text{O}$ show ditopic tetra- and penta-aza ligands can be very simply built just by introducing a *para*-substituted benzene ring into a polyamine bridge of appropriate dimensions. The low co-ordination number of these azaparcyclophanes yields distorted geometries and a considerable reduction in the stability of the copper(II) mononuclear complexes with respect to analogous saturated polyazacycloalkanes. This is reflected in interesting properties such as the stabilization of the related copper(I) complexes towards disproportion or their use in assisting hydrolytic processes. Indeed these aspects are currently under investigation and will be discussed in a future publication.

Acknowledgements

We are indebted to the Dirección General de Investigación Científica y Técnica (PB90-0567) and Institut València d'Estudis i Investigació for financial support as well as to the Italian Ministero dell'Università e della Ricerca Scientifica e Tecnologica (quota 60%).

References

- 1 K. D. Karlin and Y. Gultneh, *Prog. Inorg. Chem.*, 1987, **35**, 219; A. Nanthakumar, M. S. Nasir, K. N. Karlin, N. Ravi and B. H. Huynh, *J. Am. Chem. Soc.*, 1992, **114**, 6564; J. Ling, A. Farooq, K. D. Karlin, T. M. Loehr and J. Sanders-Loehr, *Inorg. Chem.*, 1992, **31**, 2552; I. Sanyal, M. Mahroof-Tahir, M. S. Nasir, P. Ghosh, B. I. Cohen, Y. Gultneh, R. W. Cruse, A. Farooq, K. D. Karlin, S. Liu and J. Zubieta, *Inorg. Chem.*, 1992, **31**, 4322.
- 2 See, for example, D. A. Rockliffe and A. E. Martell, *Inorg. Chem.*, 1993, **32**, 3143.
- 3 D. E. Fenton, V. Casellato, P. A. Vigato and M. Vidali, *Inorg. Chim. Acta*, 1982, **62**, 57; A. Bencini, A. Bianchi, E. Garcia-España, M. Giusti, S. Mangani, M. Micheloni, P. Orioli and P. Paoletti, *Inorg. Chem.*, 1987, **26**, 1243; B. Dietrich, M. W. Hosseini, J.-M. Lehn and R. B. Sessions, *Helv. Chim. Acta*, 1983, **66**, 1262.
- 4 R. Schneider, A. Riesen and T. A. Kaden, *Helv. Chim. Acta*, 1986, **70**, 53; E. Garcia-España, M. Micheloni, P. Paoletti and A. Bianchi,

- Gazz. Chim. Ital.*, 1985, **115**, 399; I. Murase, S. Ueno and S. Kida, *Inorg. Chim. Acta*, 1986, **111**, 57.
- 5 M. Ciampolini, L. Fabbri, A. Perotti, B. Seghi and F. Zanobini, *Inorg. Chem.*, 1987, **26**, 3527.
- 6 N. F. Curtis, *J. Chem. Soc. A*, 1968, 1584; D. Cook and E. D. Mackenzie, *Inorg. Chim. Acta*, 1978, **31**, 54; M. D. Duggan, E. K. Barefield and D. N. Hendrickson, *Inorg. Chem.*, 1973, **12**, 985; L. P. Battaglia, A. Bianchi, A. Bonamartini Corradi, E. García-España, M. Micheloni and M. Julve, *Inorg. Chem.*, 1988, **27**, 4174; A. Bencini, A. Bianchi, E. García-España, Y. Jeanin, M. Julve, V. Marcelino and M. Philoche-Levisalles, *Inorg. Chem.*, 1990, **27**, 963; A. Bencini, A. Bianchi, P. Paoli, E. García-España, M. Julve and V. Marcelino, *J. Chem. Soc., Dalton Trans.*, 1990, 2213.
- 7 A. Bencini, A. Bianchi, P. Paoletti and P. Paoli, *Coord. Chem. Rev.*, 1992, **120**, 51.
- 8 M. I. Burguete, E. García-España, S. V. Luis, J. F. Miravet and C. Soriano, *J. Org. Chem.*, 1993, **58**, 4749.
- 9 A. Andrés, M. I. Burguete, E. García-España, S. V. Luis, J. F. Miravet and C. Soriano, *J. Chem. Soc., Perkin Trans. 2*, 1993, 749.
- 10 T. Shimada, M. Kodera, H. Okawa and S. Kida, *J. Chem. Soc., Dalton Trans.*, 1992, 1121.
- 11 M. Micheloni, P. May and D. R. Williams, *J. Inorg. Nucl. Chem.*, 1978, **40**, 1209.
- 12 M. Micheloni, A. Sabatini and A. Vacca, *Inorg. Chim. Acta*, 1977, **25**, 41.
- 13 E. García-España, M.-J. Ballester, F. Lloret, J.-M. Moratal, J. Faus and A. Bianchi, *J. Chem. Soc., Dalton Trans.*, 1988, 101.
- 14 M. Fontanelli and M. Micheloni, *Proceedings of the First Spanish-Italian Congress on Thermodynamics of Metal Complexes*, Peñíscola, Castellón, Spain, 1990.
- 15 G. Gran, *Analyst (London)*, 1952, **77**, 881; F. J. Rossotti and H. Rossotti, *J. Chem. Educ.*, 1965, **42**, 375.
- 16 P. Gans, A. Sabatini and A. Vacca, *J. Chem. Soc., Dalton Trans.*, 1985, 1195.
- 17 A. Vacca, unpublished work.
- 18 A. K. Covington, M. Paabo, R. A. Robinson and R. G. Bates, *Anal. Chem.*, 1968, **40**, 700.
- 19 J. P. Hall, R. M. Izzat and J. J. Christensen, *J. Phys. Chem.*, 1963, **67**, 2605.
- 20 M. Micheloni, KK88 program (FORTRAN), Florence, 1988.
- 21 N. Walker and D. Stuart, *Acta Crystallogr., Sect. A*, 1983, **39**, 158.
- 22 G. M. Sheldrick, SHELX 76, A Program for Crystal Structure Determination, University of Cambridge, 1976.
- 23 *International Tables for X-Ray Crystallography*, Kynoch Press, Birmingham, 1974, vol. 4.
- 24 M. Bartolini, A. Bianchi, M. Micheloni and P. Paoletti, *J. Chem. Soc., Perkin Trans. 2*, 1982, 1345.
- 25 M. Kodama and E. Kimura, *J. Chem. Soc., Dalton Trans.*, 1980, 327.
- 26 M. Kodama and E. Kimura, *J. Chem. Soc., Dalton Trans.*, 1978, 104.
- 27 R. M. Smith and A. E. Martell, *Critical Stability Constants*, Plenum, New York, 1975, vol. 1; J. Aragón, A. Bencini, A. Bianchi, E. García-España, M. Micheloni and P. Paoletti, *J. Chem. Soc., Dalton Trans.*, 1991, 3077.
- 28 E. Sarneski, H. L. Surprenant, F. K. Molen and C. N. Reilley, *Anal. Chem.*, 1975, **47**, 1126.
- 29 M. Kodama and E. Kimura, *J. Chem. Soc., Dalton Trans.*, 1978, 1081.
- 30 L. Fabbri, M. Micheloni and P. Paoletti, *J. Chem. Soc., Dalton Trans.*, 1979, 1581; L. Fabbri and L. Zompa, *J. Inorg. Nucl. Chem. Lett.*, 1977, **13**, 287.
- 31 R. M. Izatt, K. Pawlak and J. S. Bradshaw, *Chem. Rev.*, 1991, **91**, 1721.
- 32 M. I. Burguete, B. Escuder, E. García-España, S. V. Luis, J. F. Miravet and C. Soriano, unpublished work.
- 33 C. K. Johnson, ORTEP, Report ORNL-3794, Oak Ridge National Laboratory, Oak Ridge, TN, 1971.
- 34 M. Nardelli, *Comput. Chem.*, 1983, **7**, 95.
- 35 C. Bazzicaluppi, A. Bencini, A. Bianchi, V. Fusi, E. García-España, P. Paoletti, P. Paoli and B. Valtancoli, *Inorg. Chem.*, 1994, **33**, 617; P. K. Coughlin and S. J. Lippard, *J. Am. Chem. Soc.*, 1984, **106**, 2328; W. F. Schwindinger, T. G. Fawcett, R. A. Lalancette, J. A. Potenza and H. J. Schugar, *Inorg. Chem.*, 1980, **19**, 1379.

Received 13th April 1994; Paper 4/02186J